Structures of the Anionic Mo/Co/S Cluster Salts $[BnNMe_3][Cp'_2Mo_2Co_2S_4(CO)_2]$, $[Na(15\text{-crown-}5)_{1.5}][Cp^*_2Mo_2Co_2S_4(CO)_2]$, and $[BnNMe_3][Cp'_2Mo_2Co_2S_3(CO)_3(SAr)]$ (Bn = Benzyl, Cp* = C_5Me_4Et, Ar = *p*-Tolyl)

M. David Curtis,* Scott H. Druker, Lukas Goossen, and Jeff W. Kampf

Department of Chemistry, Willard H. Dow Laboratory, The University of Michigan, Ann Arbor, Michigan 48109-1055

Received July 30, 1996[⊗]

The paramagnetic cluster anions $Cp'_2Mo_2Co_2S_4(CO)_2^-$ (**6**), and $Cp^*_2Mo_2Co_2S_4(CO)_2^-$ (**6***) were prepared by the reaction of $Cp'_2Mo_2Co_2S_3(CO)_4$ with *p*-toluene thiolate or by Na amalgam reduction of the cubane $Cp^*_2Mo_2Co_2S_4(CO)_2$ ($Cp^* = C_5Me_4Et$), respectively. The CO-substituted cluster $Cp'_2Mo_2Co_2S_3(CO)_3(SAr)^-$ (**7**) was a minor byproduct in the synthesis of **6**. The X-ray crystal structures of these anionic clusters were determined. The effects of the addition or removal of electron density from the cluster core on the cluster structure is presented.

Transition metal-mediated or catalyzed desulfurization reactions of organic sulfur compounds are important in organic synthetic transformations[1] and in connection with the industrially important hydrodesulfurization (HDS) process in the refinement of fossil fuels.[2] The latter process, in particular, has inspired a considerable amount of organometallic chemistry of sulfur-containing compounds, e.g., thiophenes, benzothiophenes, thiols, and cyclic sulfides.[3−8] These HDS catalysts typically consist of MoS_2 promoted with various Co salts and supported on a high surface area oxide, e.g., Al_2O_3.[2] In our laboratories, the reactions of thiols and thiolate anions with the Mo/Co/S cluster **1** have been investigated as models for desulfurizations over the industrial Co/Mo/S HDS catalyst.[9−12] In the reactions of thiols with cluster **1**, cluster **2** is formed in quantitative yields along with the hydrocarbon corresponding to the thiol (eq 1).[9]

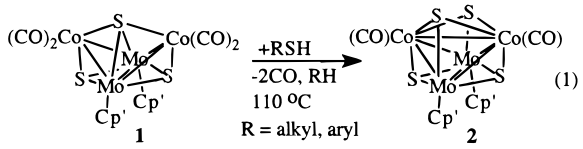

(1)

Kinetic studies have shown that the rate-determining step (rds) of the reaction shown in eq 1 is the initial coordination of the thiol to the cluster and not the scission of the C−S bond.[11] The reactions of cluster **1** with thiolate anions were studied in an attempt to change the rds from the initial coordination step to the actual C−S bond cleavage since thiolate anions are much more nucleophilic than their parent thiols. It was found that thiolate anions do indeed react rapidly with **1** according to Scheme 1. At low temperatures (≤−40 °C) the adduct **3** forms initially but rearranges to the less symmetric isomer **4** at −25 °C. Upon gentle heating, **4** underwent C−S bond homolysis and loss of carbon monoxide and formed the radical anion of cluster **2** (**6**) as the sole, organometallic product.

[⊗] Abstract published in *Advance ACS Abstracts,* December 15, 1996.

(1) (a) Wong, K. Y.; Wang, M. C.; Tung, H.; Luh, T. *J. Am. Chem. Soc.* **1994**, *116*, 8920. (b) Luh, T.-Y.; Ni, Z.-J. *Synthesis* **1990**, 89.

(2) (a) Topsøe, H.; Clausen, B. S.; Massoth, F. E. Reprinted from *Catalysis-Science and Technology*; Anderson, J. R., Boudart, M., Eds.; Springer-Verlag: New York, **1996**, Vol. 11. (b) Chianelli, R. R.; Daage, M.; Ledoux, M. J. *Adv. Catal.* **1994**, *40*, 177−232. (c) Hoffman, H. L. *Hydrocarbon Processing* **1991**, *70*, 37. (d) Massoth, F. E. *Adv. Catal.* **1978**, *27*, 265.

(3) (a) Angelici, R. J. *Acc. Chem. Res.* **1988**, *21*, 387. (b) Benson, J. W.; Angelici, R. J. *Organometallics* **1993**, *12*, 680. (c) Sauer, N. N.; Markel, E. J.; Schrader, G. L.; Angelici, R. J. *J. Catal.* **1989**, *117 (1)*, 295−7. (d) Robertson, M. J.; Day, C. L.; Jacobson, R. A.; Angelici, R. J. *Organometallics* **1994**, *13*, 179. (e) Chen, J.; Daniels, L. M.; Angelici, R. J. *Organometallics* **1996**, *15*, 1223. (f) Chen, J.; Young, V. G. J.; Angelici, R. J. *Organometallics* **1996**, *15*, 1414.

(4) (a) Rauchfuss, T. B., *Prog. Inorg. Chem.* **1991**, *39*, 260. (b) Luo, S.; Rauchfuss, T. B.; Gan, Z. *J. Am. Chem. Soc.* **1993**, *115*, 4943. (c) Luo, S.; Ogilvy, A. E.; Rauchfuss, T. M.; Rheingold, A. L.; Wilson, S. R. *Organometallics* **1991**, *10*, 1002. (d) Krautscheid, H.; Feng, Q.; Rauchfuss, T. B. *Organometallics* **1993**, *12*, 3273. (e) Feng, Q.; Krautscheid, H.; Rauchfuss, T. R.; Skaugset, A. E.; Venturelli, A. *Organometallics* **1995**, *14*, 297−304.

(5) (a) Bianchini, C.; Meli, A. *J. Chem. Soc., Dalton Trans.* **1996**, 801. (b) Bianchini, C.; Meli, A.; Perizzini, M.; Vizza, F.; Herrera, V.; Sanchez-Delgado, R. A. *Organometallics* **1994**, *13*, 721. (c) Bianchini, C.; Meli, A.; Peruzzini, M.; Vizza, F.; Moneti, S.; Herrera, V.; Sanchez-Delgado, R. A. *J. Am. Chem. Soc.* **1994**, *116*, 4370. (d) Bianchini, C.; Jimenez, M. V.; Meli, A.; Moneti, S.; Vizza, F.; Herrera, V.; Sanchez-Delgado, R. A. *Organometallics* **1995**, *14*, 2342.

(6) (a) Myers, A. J.; Jones, W. D.; McClements, S. M. J. *Am. Chem. Soc.* **1995**, *117*, 11704. (b) Jones, W. D.; Chin, R. M. *J. Am. Chem. Soc.* **1994,** *116*, 198. (c) Jones, W. D.; Chin, R. M. *Organometallics* **1992**, *11*, 2698. (d) Rosini, C. P.; Jones, W. D. *J. Am. Chem. Soc.* **1992**, *114*, 10767. (e) Dong, L.; Duckett, S. B.; Ohman, K. F.; Jones, W. D. *J. Am. Chem. Soc.* **1992**, *114*, 151. (f) Jones, W. D.; Chin, R. M. *J. Am. Chem. Soc.* **1992**, *114*, 9851.

(7) (a) Rakowski Du Bois, M. *Chem. Rev.* **1989**, *89*, 1. (b) Bernatis, P.; Haltiwanger, R. C.; Rakowski Dubois, M. *Organometallics* **1992**, *11*, 2435.

(8) (a) Adams, R. D. *Chem. Rev.* **1995**, *95*, 2587. (b) Adams, R. D.; Horvath, I. T. *Prog. Inorg. Chem.* **1985**, *33*, 127. (c) Adams, R. D.; Pompeo, M. P.; Wu, W.; Yamamoto, J. H. *J. Am. Chem Soc.* **1993**, *115*, 8207 and references therein. (d) Adams, R. D. *Polyhedron* **1985**, *4 (12)*, 2003−26. (e) Adams, R. D.; Pompeo, M. P.; Wu, W.; Yamamoto, J. H. *J. Am. Chem. Soc.* **1993**, *115*, 8207.

(9) (a) Riaz, U.; Curnow, O.; Curtis, M. D. *J. Am. Chem. Soc.* **1994**, *116*, 4357. (b) Riaz, U.; Curnow, O.; Curtis, M. D. *J. Am. Chem. Soc.* **1991**, *113*, 1416.

(10) Curtis, M. D.; Penner-Hahn, J. E.; Schwank, J.; Baralt, O.; McCabe, D. J.; Thompson, L.; Waldo, G. *Polyhedron* **1988**, *7*, 2411.

(11) (a) Druker, S. H.; Curtis, M. D. *J. Am. Chem. Soc.* **1995**, *117*, 6366. (b) Curtis, M. D.; Druker, S. H. *J. Am. Chem. Soc.*, in press.

(12) Curtis, M. D. *ACS Symposium Series*; Stiefel, E. I., Matsumoto, K., Eds.; American Chemical Society: Washington, DC, in press.

S0276-7333(96)00633-4 CCC: $14.00

Scheme 1

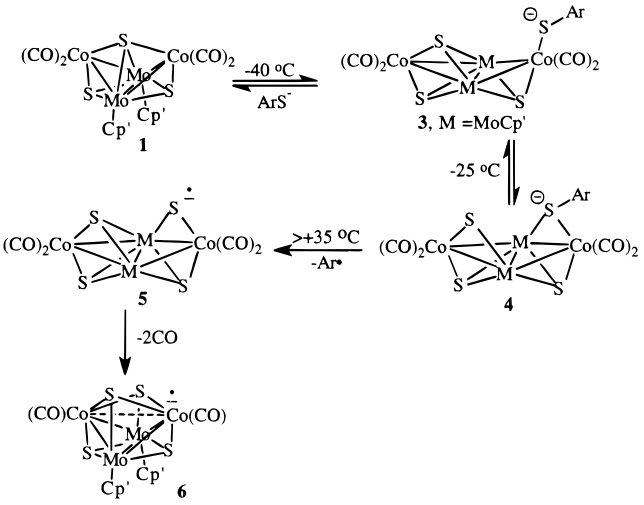

In this note, we describe the independent synthesis and structure of a complex that contains a radical cluster anion with substituted Cp groups (**6***, Cp = Cp^{Et} = C_5Me_4Et), the structure of the benzyltrimethylammonium salt of anion **6**, and that of the CO-substituted anionic cluster **7**. The latter compound is formed in trace amounts during the synthesis of the adduct **4** (eq 2). The structure of **6** has been communicated previously.[11a]

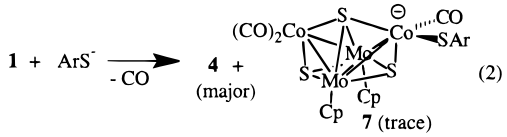

Experimental Section

Reduction of $Cp^{Et}_2Mo_2Co_2S_4(CO)_2$ (2*, Cp^{Et} = C_5Me_4Et) with Sodium Amalgam. A 25 mL Schlenk flask was charged with an excess amount of 0.3% Na amalgam. A solution of **2*** (100 mg, 0.15 mmol) in THF was added to the amalgam, and the mixture was stirred for 30 min. The solution was removed via cannula, and four drops of 15-crown-5 was added. The solvent was removed under vacuum, and the dark residue was washed with 1 mL of ether. The remaining solid was suspended in 5 mL of toluene, and sufficient acetonitrile was added to just dissolve the solid. This solution was filtered through a fine frit into a vial which was placed in the inert-atmosphere box, and the solvent was allowed to slowly evaporate to give dark green crystals (64 mg, 44% yield based on $[Na(15\text{-crown-}5)_{1.5}][Cp^{Et}_2Mo_2Co_2S_4(CO)_2]$ (Na(**6***)), the formula established by a solution of the X-ray diffraction data). IR (CH_3CN) (ν(CO)): 1902 and 1873 cm^{-1}. The extreme oxygen sensitivity of Na(**6***) prevented its accurate elemental analysis.

Synthesis of $[BnNMe_3][Cp'_2Mo_2Co_2S_4(CO)_2]$ ($BnNMe_3$(6)) (Bn = benzyl). This compound was made by the thermal decomposition of the thiolate adduct, $[BnNMe_3][Cp'_2Mo_2Co_2S_3(CO)_2SAr]$ (Cp′ = C_5H_4Me, Ar = *p*-tolyl) formed from cluster **1** (50 mg, 0.074 mmol) and $[BnNMe_3][SAr]$ (45 mg, 0.15 mmol) in 25 mL of acetonitrile. ($[BnNMe_3][SAr]$ was prepared by the metathesis of $[BnNMe_3]Cl$ and NaSAr in ^{i}BuOH.) This solution of the adduct was heated to 80 °C for 1 h, after which time a ^{1}H-NMR spectrum of a sample of the mixture indicated complete conversion of starting material according to Scheme 1. The solution was concentrated and layered with diethyl ether and allowed to stand. Dark green-black crystals of the product formed and were collected by filtration. IR (CH_3CN), (ν_{CO}): 1898 and 1865 cm^{-1}.

Isolation of $[BnNMe_3][Cp'_2Mo_2Co_2S_3(CO)_3(SAr)]$ (Ar = *p*-Tolyl, 7). A 25 mL Erlenmeyer flask was charged with cluster **1** (50 mg, 0.074 mmol) and $[BnNMe_3][SC_6H_5CH_3]$ (45 mg, 0.15 mmol). Acetonitrile (4 mL) was added, and the solution was stirred for 1 h. The solution was filtered and then layered with diethyl ether to induce crystallization. Dark green crystals ($BnNMe_3$ salt of cluster anion **4**; see Scheme 1) were obtained (32 mg). Anal. Calcd for $C_{33}H_{37}Co_2Mo_2NO_4S_4$: C, 41.70; H, 4.05; N, 1.52. Found: C, 42.51; H, 4.10; N, 1.46. IR (CH_3CN) (ν(CO)): 1962 and 1913 cm^{-1}. ^{1}H-NMR at 295 K (CD_3CN): bound thiolate, δ 7.34 (d, 2H), 6.82 (d, 2H), 2.22 (s, 3H); cation, δ 7.54 (m, 5H), 4.37 (s, 2H), 2.98 (s, 9H); CpH, δ 5.50 (m, 2H) plus three additional broad peaks between 4.9 and 6.0 ppm; $CpCH_3$, δ 2.04 (s, 6H). A microscopic examination of this batch of crystals revealed several, larger, well-formed crystals that were selected for X-ray diffraction analysis. Subsequent solution and refinement of the structure showed that these larger crystals were the $BnNMe_3$ salt of the CO-substituted product, **7**. Deliberate attempts to maximize the yield of **7** by heating or photolysis of solutions of **4** invariably resulted in the desulfurization reaction shown in Scheme 1 and isolation of salts of the cubane radical anion, **6**.

Molecular Structure of $[BnNMe_3][Cp'_2Mo_2Co_2S_4(CO)_2]$ ($BnNMe_3$(6)). Crystal, data collection, and refinement parameters are tabulated in Table IS (Supporting Information). A black rectangular crystal was sealed in a glass capillary and mounted on a Siemans R3m/v diffractometer, equipped with a low-temperature apparatus. The unit cell dimensions were obtained from the least-squares fit of 29 reflections (16.3° ≤ 2θ ≤ 29.1°). The space group was chosen as $P\bar{1}$ (No. 2). The number of data collected was 4074 with 3417 unique reflections. A semi-empirical absorption correction (XABS2: Parkin, S. Ph.D. Thesis, University of California, Davis, CA, 1993) was applied to the data. The structure was solved by the direct methods. All non-hydrogen atoms were refined anisotropically, while the hydrogen atoms were fitted using the riding model (d_{C-H} = 0.94 Å, U(H) = 0.153(4)). The final structural model had GOF = 1.091, R = 0.0354, R_w = 0.0938, and a data/parameter ratio = 10. The routines used for the structure solution and refinement were the Siemans SHELXTL PLUS and SHELXL-93 running on a VAX Station 3500. Table IIS contains positional parameters for the non-hydrogen atoms, and Table IIIS contains positional parameters for the hydrogen atoms. Anisotropic temperature factors are in Table IVS.

Molecular Structure of $[BnNMe_3][Cp'_2Mo_2Co_2S_3(CO)_3SAr]$ ([$BnNMe_3$]7, Ar = $C_6H_4CH_3$). A black, flat needle was sealed in a glass capillary and mounted on a Nicolet R3 diffractometer. Crystal, data collection, and refinement parameters are tabulated in Table VS. The unit cell dimensions were obtained from the least-squares fit of 25 reflections (12.6° ≤ 2θ ≤ 26.5°). The space group was chosen as $P\bar{1}$ (No. 2). The number of reflections collected was 8814. An empirical absorption correction was applied to the data. The structure was solved by direct methods. All non-hydrogen atoms were refined anisotropically, while the hydrogen atoms were fitted using the riding model (aromatic H, d_{C-H} = 0.95 Å; aliphatic H, d_{C-H} = 0.98 Å). The final structural model had GOF = 1.097, R = 0.0487, R_w = 0.1242, and data/parameter ratio = 10.3. Table VIS contains positional parameters for the non-hydrogen atoms, and Table VIIS contains positional parameters for the hydrogen atoms. Anisotropic temperature factors are in Table VIIIS.

Molecular Structure of $[Na(15\text{-crown-}5)_{1.5}][Cp^{Et}_2Mo_2Co_2S_4(CO)_2]$ (Na(6*)). A black, rectangular plate was sealed in a glass capillary and mounted on a Syntex $P2_1/c$ diffractometer. Crystal, data collection, and refinement parameters are located in the Supporting Information. The unit cell dimensions were obtained from the least-squares fit of 33 reflections (10.5° ≤ 2θ ≤ 30.0°). The space group was chosen as $P2_1/c$ (No. 14), Z = 4. The number of reflections collected was 9434 with 7858 being unique. A semi-empirical absorption correction (ψ scan) was applied to the data. The structure was solved

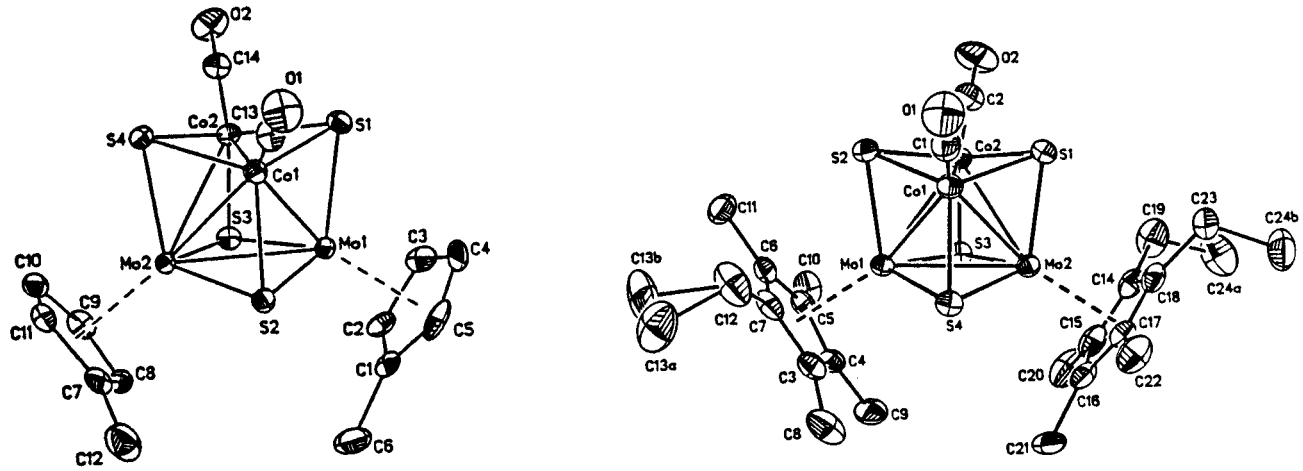

Figure 1. Left: ORTEP drawing of the anion **6**. Right: ORTEP drawing of the anion **6***. Thermal ellipsoids are drawn at the 50% probability level.

by locating the Mo positions in a Patterson map, and the remaining non-hydrogen atoms were located in subsequent difference maps. All non-hydrogen atoms were refined anisotropically, except those in the disordered crown ether and the disordered Cp* groups (see below). The hydrogen atoms, placed in calculated positions, were not used in the refinement, but their contribution to the scattering was included in the final calculation. The final structural model had GOF = 1.097, $R = 0.0487$, $R_w = 0.1242$, and data/parameter ratio = 10.3. Table XS contains positional parameters for the non-hydrogen atoms, and Table XIS contains positional parameters for the hydrogen atoms. Anisotropic temperature factors are in Table XIIS.

Results and Discussion

Cubane Structures. The ORTEP drawings of the cubane clusters, **6** and **6***, are shown in Figure 1. Complete tables of bond distances and angles are given in the Supporting Information. The benzyltrimethylamonium salt of **6** was obtained from the "decomposition" of the adduct of [BnNMe$_3$][SAr] (Ar = *p*-tolyl) according to Scheme 1. The reduction of cubane **2** with sodium amalgam also gives the anion **6**, as shown by the appearance of the characteristic υ_{CO} bands at 1898 and 1965 cm^{-1} (in THF) in the IR spectrum. However, we were unable to grow large or well-formed crystals from these solutions.

Sodium amalgam reduction of the substituted analog, $Cp_2^{Et}Mo_2Co_2S_4(CO)_2$, followed by addition of 15-crown-5, did allow for the growth of suitable crystals that were found to have the formula [Na(15-crown-5)$_{1.5}$][**6***] upon solution of the X-ray diffraction pattern. Two sodium ions are bound by three crown ethers across an inversion center. One crystallographically independent crown ether is relatively well behaved with 5 Na-O contacts in the range 2.50−2.68 Å. The second ether bridges the two inversion related Na ions with the inversion center in the center of the crown ether ring. The crown ether molecule is therefore required to be crystallographically disordered. It appeared that several atomic scatterers contained contributions from both carbon and oxygen, but it was not possible to determine the occupancy ratios. Hence, no attempt was made to distinguish carbon and oxygen. All atoms in the bridging ether were refined with carbon scattering factors. The atoms of both crown ethers were refined with isotopic temperature factors, and their hydrogen atoms were not included in the refinement. Figure 2 shows the packing of the Na−crown ether complex.

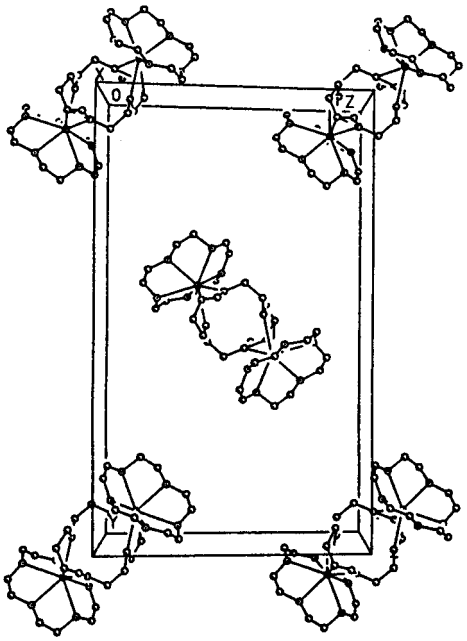

Figure 2. ORTEP drawing of the packing of the Na$_2$(15-crown-5)$_3$ complex cation.

The Cp^{Et} group also shows some disorder. The terminal carbon atom of the ethyl group of Cp1 is disordered over two positions with 50% occupancy. These two positions were labeled Cl3a and Cl3b. Both carbon atoms of the ethyl group on the second Cp^{Et} group are disordered over two positions causing the appearance of two ethyl groups with 50% occupancy. (C19, C24a, C23, C24b; Figure 1).

Table 1 lists the average metal−metal and metal−sulfur distances in the neutral cubane, **2**,[13] an oxidized cubane with 58 valence shell electrons (VSE), $Cp_2^{Et}Mo_2Co_2S_4I_2$ (**8**),[14] the 62 VSE cluster, $Cp'_2Mo_2Ni_2S_4(CO)_2$ (**9**),[15] and the 61 VSE anions **6** and **6***. These structures show a very regular set of dimensions, with the ranges

(13) Curtis, M. D.; Riaz, U.; Curnow, O. J.; Kampf, J. W.; Rheingold, A. L.; Haggerty, B. J. *Organometallics* **1995**, *14*, 5337.
(14) Mansour, M. A.; Curtis, M. D.; Kampf, J. W. *Organometallics* **1995**, *14*, 5460.
(15) Curtis, M. D.; Williams, P. D.; Butler, W. M. *Inorg. Chem.* **1988**, *27*, 2853.

Table 1. Average Metal−Metal and Metal−Sulfur Distances (Å) in Clusters 2, 8, 9, 6, and 6*

bond[a]	**2**[b]	**8**[c]	**9**[d]	**6**	**6***	Δ_{max} (Å)
M′-M′	2.571(1)	2.936(1)	2.960(2)	2.746(1)	2.735(1)	0.39
Mo−Mo	2.831(1)	2.803(1)	2.829	2.838(1)	2.846(1)	0.05
Mo−M′	2.712(4)	2.738(5)	2.722(2)	2.739(9)	2.731(6)	0.03
Mo−S	2.328(4)	2.32(2)	2.30(4)	2.33(1)	2.33(2)	0.03
M′−S	2.21(2)	2.24(2)	2.24(6)	2.22(4)	2.21(3)	0.03

[a] M′ = Co for clusters **2**, **8**, **6**, and **6***; M′ = Ni for **9**. [b] Calculated from data in ref 13. [c] Calculated from data in ref 14. [d] Calculated from data in ref 15.

in distances varying between 0.03 and 0.05 Å. The sole exception is the Co−Co distance in which a variation of nearly 0.4 Å is observed.

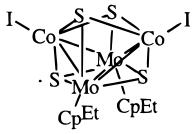

8

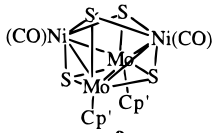

9

In the neutral, 60 VSE cluster **2**, there are nominally 6 metal−metal bonds,[16−19] and a bond order of 1.0 is assigned to the Co−Co bond. In the Mo_2Ni_2 cluster **9**, there are 62 VSE appropriate for a "butterfly" type of cluster with 5 metal−metal bonds. Accordingly, the long Ni−Ni distance, 2.96 Å, represents a nonbonded separation in this "cubane−butterfly". Unlike most butterfly clusters in which the wing-tips are not tethered together and the wings can open fully (even to a planar structure), the μ_3-bridging S atoms in the cubane clusters restrict the separation of the wing-tip metals. As the metal−metal distance increases, the two bridging sulfur atoms are pulled together if the M−S bond distance is maintained. Eventually, the S···S contact becomes so repulsive that the M···M distance is limited to about 3 Å for a M−S distance of 2.2 Å. The iodo-substituted cluster, **8**, is obtained from the dicarbonyl cubane **2*** by oxidation with iodine. This cluster has 58 VSE. The Co···Co distance, 2.94 Å, is nonbonding. Thus, upon oxidation, the two electrons appear to have been removed from a Co−Co bonding molecular orbital (MO).

The Co−Co distances found in the 61 VSE electron radical anions, **6** and **6***, are 2.75 and 2.74 Å, respectively. These distances are almost exactly halfway between the fully bonded distance, 2.57 Å, in **2** and the nonbonded distances in **8** and **9**. Thus, it appears that the "extra" electron in **6** or **6*** is added to a Co−Co σ*-MO to give a bond order of 0.5. Support for this interpretation is found in the ESR spectrum of **6*** which is consistent with the odd electron being delocalized over 2 Co atoms, each with spin $I = {}^7/_2$ (13 of the expected 15 lines were observed; the outer ones were too weak). The measured g-value is 2.03, and the hyperfine splitting is $A = 13.2$ g. Addition of another electron, as in **9**, reduces the bond order to zero.

Interestingly, the Co−Co distances in **6** and **6*** are almost identical to the Co−Co distance in $Cp'_2V_2Co_2S_4(NO)_2$ (**10**), 2.738(1) Å.[19] The latter compound is a rare example of a paramagnetic ($S = 1$), 60 VSE cluster. Thus, it appears that in **10** there is one electron each in a Co−Co bonding MO and a nonbonding or weakly antibonding MO to give a net Co−Co bond order of 0.5. Rauchfuss et al. have also reported a very short Fe−Fe bond distance (2.590(1) Å) in the 58 VSE, antiferromagnetic cluster $Cp'_2V_2Fe_2S_4(NO)_2$ (**11**).[19] However, in contrast to the Mo clusters reported here, it is the V−V distance in **11** that appears elongated (2.957(1) Å) as a result of the decrease in electron count.

With these structural results in hand, it is tempting to conclude that, in $Mo_2M'_2S_4$ clusters (M = Fe, Co, Ni), the HOMO is M′−M′ σ-bonding and the LUMO is M′−M′ σ*-antibonding, whereas, in Rauchfuss' $V_2M'_2$ clusters, the HOMO is V−V σ-bonding but the LUMO is M′−M′ σ*-antibonding. The actual situation may not be that simple. It is generally agreed that, in M_4S_4 clusters with T_d symmetry, the LUMO is a triply degenerate MO with metal−metal antibonding character and that the occupied frontier orbitals consist of a set of six orbitals (a_1, e, and t_2). The a_1 and e symmetry MO's have M−M bonding character, and the t_2-symmetry electrons are essentially nonbonding.[16−18] In bimetallic clusters, the symmetry is broken and the degeneracies are reduced or removed. However, the basic character of the orbitals should not change too much. For example, the 58 VSE cluster $Cp_3Mo_3FeS_4(SH)$, with C_{3v} symmetry, may have doubly degenerate orbitals, and this cluster exhibits Mo−Mo and Mo−Fe distances that are appropriate for bond orders of unity; i.e., the removal of two electrons from the M−M bonding manifold is not expressed in structural distortions.[13] In the C_{2v} symmetry $Mo_2M'_2$ clusters, on the other hand, deviation of the electron count from 62 is expressed as an increase in the M′−M′ distance. While these observed distortions are consistent with M′−M′ bonding and antibonding character for the HOMO and LUMO, respectively, in the 60 VSE cluster, one must also realize that the energy of the $\sigma_{M'M'}$ will increase and that of the $\sigma^*_{M'M'}$ will decrease as the M′−M′ distance increases. Hence, the $\sigma_{M'M'}$ and $\sigma^*_{M'M'}$ orbitals are not necessarily the HOMO and LUMO in the M′−M′-bonded, 60 VSE cluster, since the observed structures are those that minimize the *total* electronic energy.

Thiolato Cluster 7. The complex **7** formed in a trace amount during the synthesis of **4** (Scheme 1). The bulk sample from which a crystal of **7** was isolated analyzed well (elemental analysis, ESI-MS, ^{1}H-NMR) for the simple adduct $[BnNMe_3][Cp'_2Mo_2Co_2S_3(CO)_4SAr]$ (Ar = p-$C_6H_4CH_3$) (**4**). Since **4** and **7** differ in composition only by the presence or absence of a carbonyl group, a structure determination was deemed necessary. Once the identity of **7** was established, attempts to directly synthesize it were unsuccessful: photolysis of **4** resulted in complete degradation, and heating a solution **4**, prepared from a mixture of **1** and $[BnNMe_3][SC_6H_4CH_3]$, resulted in the desulfurization of the thiolate as shown in Scheme 1.[11]

In Table 2, the bond distances of the cluster $Cp'_2Mo_2Co_2S_3(CO)_4$ (**1**), are compared with those of the derivative **7** in which a carbonyl group is replaced by the ArS^- thiolato ligand. Figure 3 shows the ORTEP plot of the structure. There is remarkably little perturbation of the bond distances in the cluster core as a result of the

(16) Williams, P. D.; Curtis, M. D. *Inorg. Chem.* **1986**, *25*, 4562.
(17) Harris, S. *Polyhedron* **1989**, *8*, 2843.
(18) Davies, C. E.; Green, J. C.; Kaltsoyannis, N.; MacDonald, M. A.; Qin, J.; Rauchfuss, T. B.; Redfern, C. M.; Stringer, G. H.; Woolhousse, M. G. *Inorg. Chem.* **1992**, *31*, 3779.
(19) (a) Rauchfuss, T. B.; Gammon, S. D.; Weatherill, T. D.; Wilson, S. R. *New J. Chem.* **1988**, *12*, 373. (b) Rauchfuss, T. B.; Weatherill, T. D.; Wilson, S. R. Zebrowski, J. P. *J. Am. Chem. Soc.* **1983**, *105*, 6508.

Table 2. Selected Bond Distances in Clusters 1 and 7

bond	**1**[a]	**7**
Co1−S1	2.199(2)	2.178(2)
Co1−S3	2.239(2)	2.284(2)
Co2−S2	2.194(2)	2.206(2)
Co2−S3	2.234(2)	2.245(2)
Co1−Mo1	2.635(1)	2.676(1)
Co1−Mo2	2.651(1)	2.701(1)
Co2−Mo1	2.635(1)	2.652(1)
Co2−Mo2	2.656(1)	2.663(1)
Mo1−S1	2.362(2)	2.354(2)
Mo1−S2	2.362(2)	2.398(2)
Mo1−S3	2.390(2)	2.417(2)
Mo2−S1	2.354(2)	2.383(2)
Mo1−S2	2.351(2)	2.374(2)
Mo1−S3	2.402(2)	2.381(2)
Mo1−Mo2	2.646(1)	2.676(1)
Co1−S4		2.272(2)

[a] Calculated from the data in ref 15.

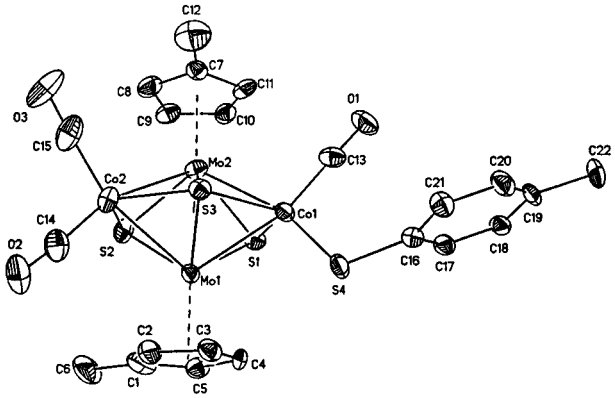

Figure 3. ORTEP drawing of the anion **7**. Thermal ellipsoids are drawn at the 50% probability level.

substitution of the π-acid carbonyl ligand with the π-donor thiolate. However, there is a slight expansion of the cluster core in **7** relative to that in **1**, since the M−M and M−S bond distances are all about 0.02 Å longer in the former. The largest changes are seen in the Co1−Mo and Co1−S bonds as might be expected. The mean Co1−Mo distance in **7** is 2.69(1) Å vs 2.64(1) Å in **1**. The Co2−Mo bond length, at 2.66 (1) Å, is intermediate between these two extremes. In **7**, the Co−S(μ_3) length is 2.19 (2) Å and the Co-S(μ_4) distance is 2.26 (3) Å, a difference of 0.07 Å. In **1**, the corresponding distances are Co−S(μ_3) = 2.20(1) Å and Co−S(μ_4) = 2.24 (1) Å, a difference of only 0.04 Å.

In both **1** and **7**, the Mo−Mo bond distances are anomalously short when compared to the Mo−Co bond lengths. The average Mo−Co bond distances in **1** and **7** are 2.64 (1) and 2.67 (2) Å, respectively. The difference in the covalent radii of Mo and Co is expected to be about 0.16 Å, and indeed, this difference is seen in the average Mo−S and Co−S bond lengths (2.39(3) Å vs 2.22(5) Å, respectively, for **7**). Hence, the expected Mo−Mo bond length is ca. 2.81 Å (d_{Mo-Co} + 0.16). However, the observed Mo−Mo distances, 2.646(1) and 2.676(1) Å in **1** and **7**, respectively, hardly differ from the Mo−Co bond lengths. This contraction of the Mo−Mo bond has been attributed to the effects of the bridging sulfido ligands that populate orbitals having some Mo−Mo π-bonding character.[15]

Acknowledgment. This work was supported by grants from the National Science Foundation (CHE-9205018 and CHE-9523056).

Supporting Information Available: Tables IS−XVIIS (complete crystallographic details, atomic coordinates, temperature factors, bond distances and angles) and ORTEP drawings with numbering schemes for $BnNMe_3$(**6**), Na(**6***),, and $BnNMe_3$(**7**) (32 pages). Ordering information is given on any current masthead page.

OM960633F